Electronic Supplementary Material (ESI) for Chemical Science.

Supporting Information

Synthesis of 'Reactive' and Covalent Polymeric Multilayers Coatings with Durable Superoleophobicity and Superoleophilicity Properties under Water

Dibyangana Parbat and Uttam Manna*

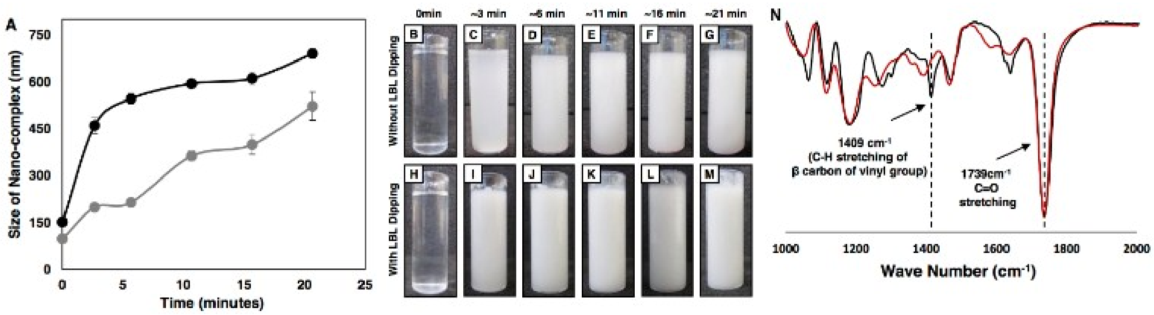

Fig. S1 A) The DLS plot showing the growth of nano-complex with time in BPEI/5Acl mixture in ethanol during LbL deposition (black) and without LbL deposition (grey) process. B-M) Digital images showing the change in appearance of BPEI/5Acl mixture with time in ethanol without LbL dipping process (B-G) and during LbL deposition process (H-M). N) FTIR spectra of nano-complex before (black) and after (red) post-chemical-functionalization with propylamine.

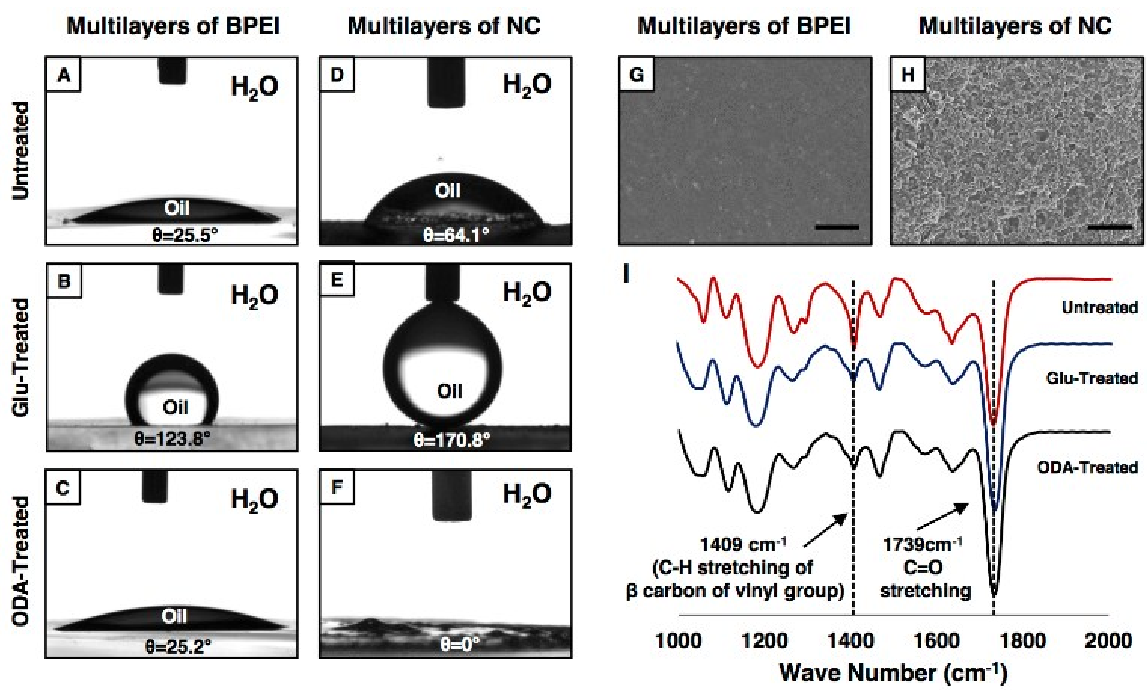

Fig. S2 A-F) OCA images showing the wetting of model oil (DCM) droplet on multilayer that are consisted of BPEI/5AcI (A-C) and NC/BPEI (D-F) before (A,D) and after (B-C, E-F) post chemical modification with glucamine (B,E) and ODA (C,F). G-H) FESEM images (scale bar = 2μm) of the multilayer that are consisted of BPEI/5AcI and NC/BPEI. I) Comparative FTIR study on untreated (red), glucamine treated (Blue) and ODA treated (black) multilayer of NC.

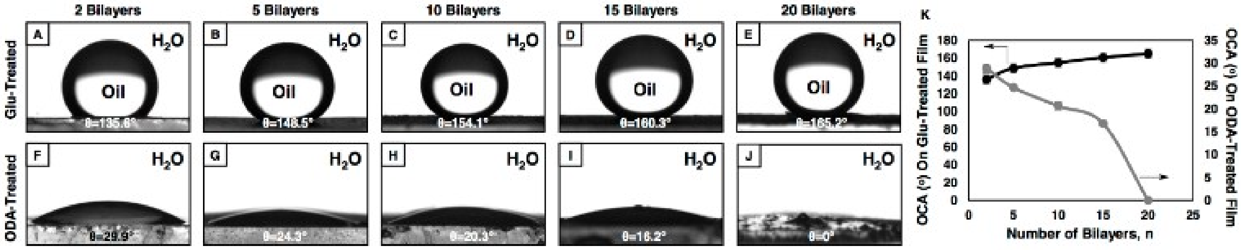

Fig. S3 A-J) Contact angle images showing the change in static-OCA of beaded oil droplets on post-modified (A-E: glucamine; F-J: octadecylamine) multilayer of NC with increasing the LbL deposition cycles. K) The plot further depicted the pattern of the change in wetting of oil on chemically-post modified multilayer of BPEI/NC under water.

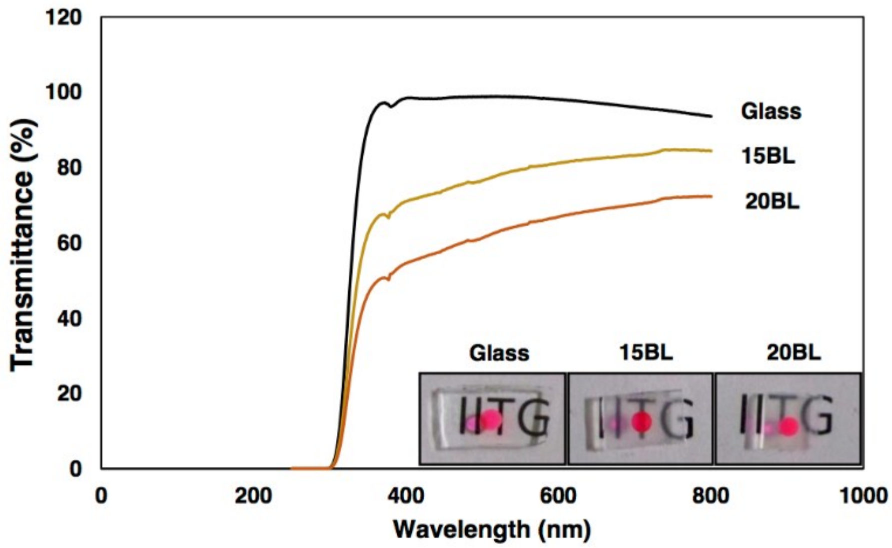

Fig. S4 The plot accounts the percentage of transmittance of uncoated (black) and multilayer coated (15 bilayer: yellow, 20 bilayer: red; both the multilayer of NC are post functionalized with glucamine) glass substrates.

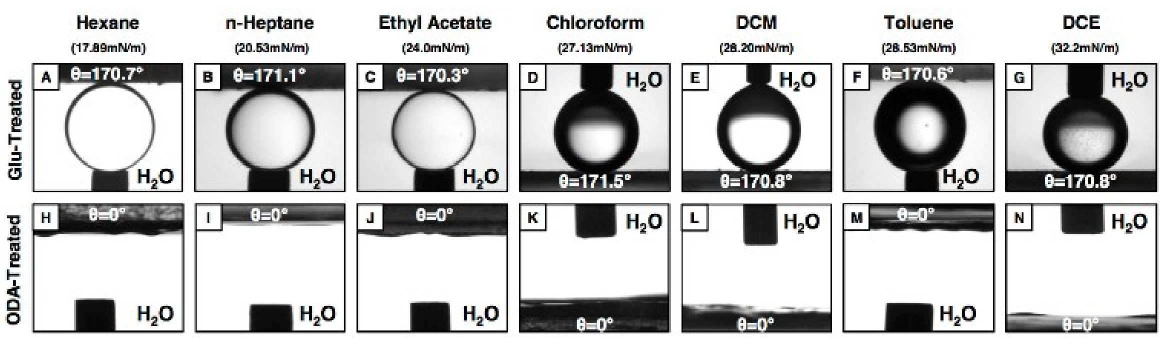

Fig. S5 A-N) Various water immiscible organic solvents are beaded on the post functionalized (glucamine and octadecylamine) multilayer coated glass substrates. All the water-immiscible liquids are extremely repelled by glucamine treated multilayer of NC, in contrast, ODA-treated multilayer readily soaked wide range of beaded droplets. The surface tensions of the selected model oils are varied from 17.89 mN/m (hexane) to 32.2 mN/m (DCE).

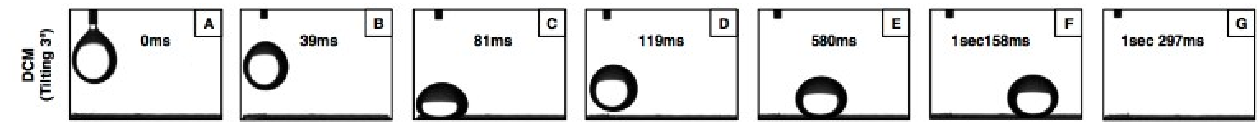

Fig. S6 A-G) Contact angle images illustrated the bouncing (A-E) and followed by rolling of (E-G) the beaded DCM droplet (11µl) on under-water superoleophobic surface—which is tilted at 3°.

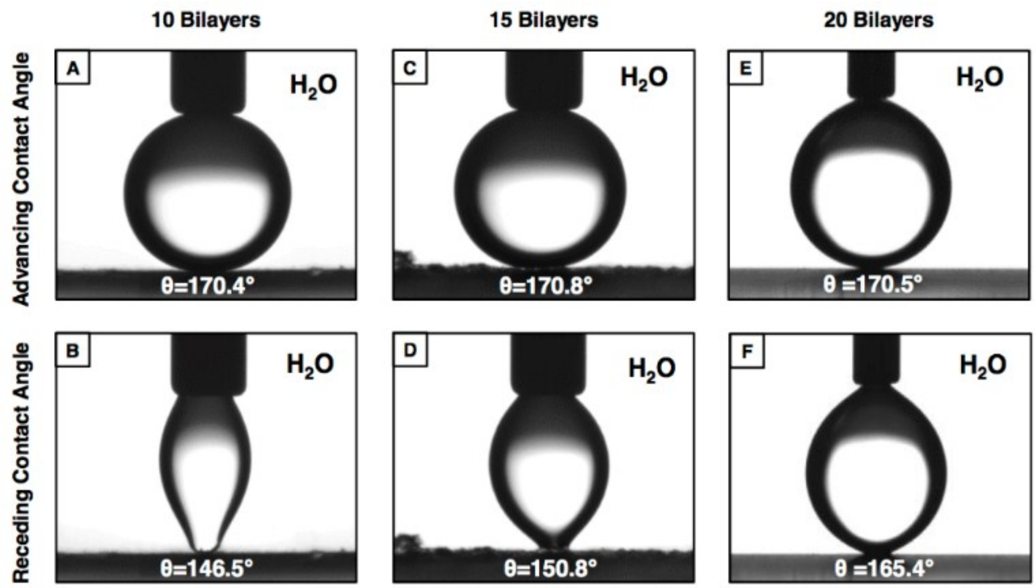

Fig. S7 A-F) The oil contact angle images showing advancing (A,C,E) and receding- (B,D,F) contact angle of beaded oil droplets on 10 bilayers, 15bilayers and 20 bilayers of nano-complex/BPEI respectively, after post-chemical-modification with glucamine.

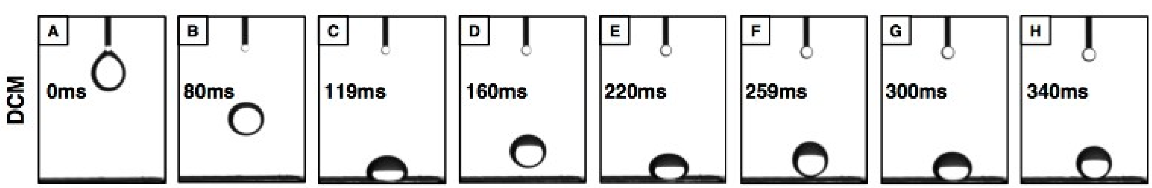

Fig. S8 A-H) Contact angle images showing the bouncing of model-oil (DCM; 11µl) droplet on a flat (no tilting) multilayer (20 bilayers, glucamine-treated) coated glass substrate.

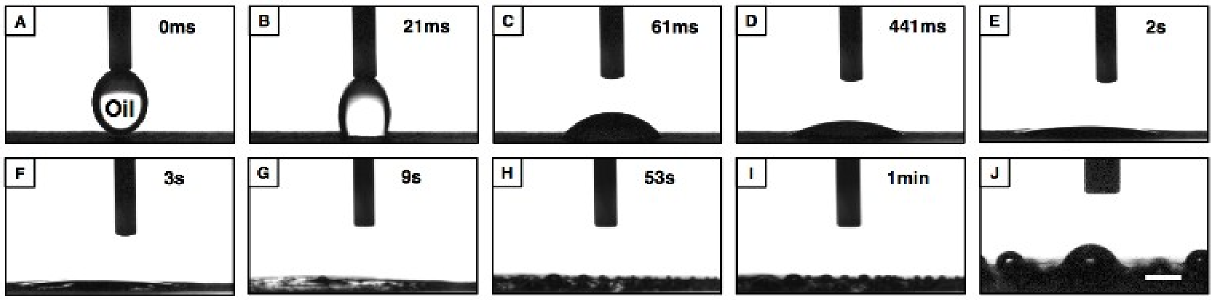

Fig. S9 A-J) Contact angle images showing beading (A-B) and wetting (C-G) of DCM on ODA-treated multilayer (20 bilayers) of nano-complexes, and the release (H-J) of trapped air from the bulk of the material to its surface over the time. J) Magnified digital image (scale bar: 500µm) of released trapped air of the surface of the multilayered coating.

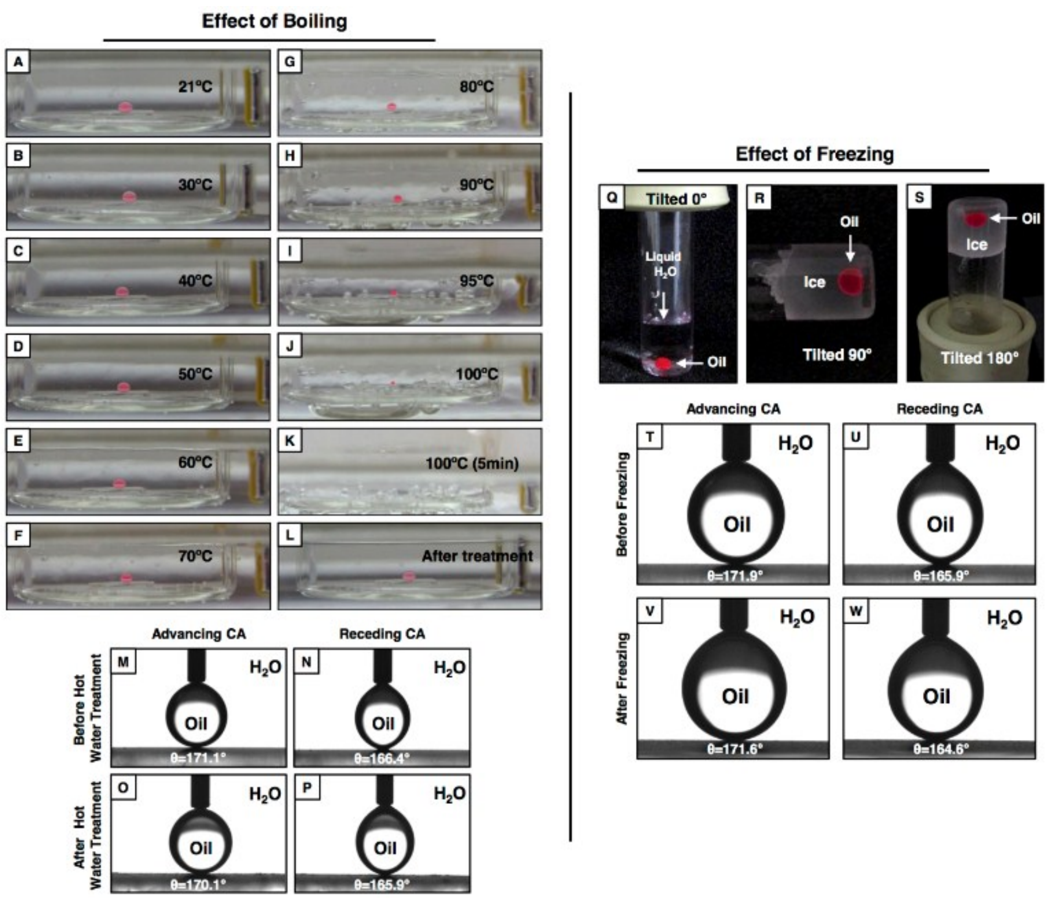

Fig. S10 A-K) Illustrating the effect of the elevated temperature of aqueous phase on the under-water wetting property of the beaded oil droplet on the glucamine-modified multilayer of NC, the temperature was raised from ambient condition (21°C, A) to boiling temperature (100°C, J-K), the size of the droplet shrinks (A-J) with increasing the temperature, however, the shape of the beaded droplet remained spherical due to extreme repulsion from glucamine-modified multilayer of NC before complete vaporization (J-K) of beaded DCM (model oil) droplet at 100°C. L) The under-water anti-oil-wetting property of the multilayer coating observed to be intact even after cooling down the aqueous phase to room temperature. M-P) Advancing (M,O) and receding (N,P) contact angles of beaded oil droplets on multilayer before (M-N) and after (O-P) heat treatment respectively. Q-S) Digital images of beaded oil droplets before (Q) and after (R-S) freezing (-20°C) the aqueous phase, the oil beaded substrate with frozen aqueous phase was tilted at 90° (R) and 180° (S). T-W) Advancing (T,V) and receding (U,W) contact angle images of beaded oil droplet before (T-U) and after (V-W) freezing treatment.

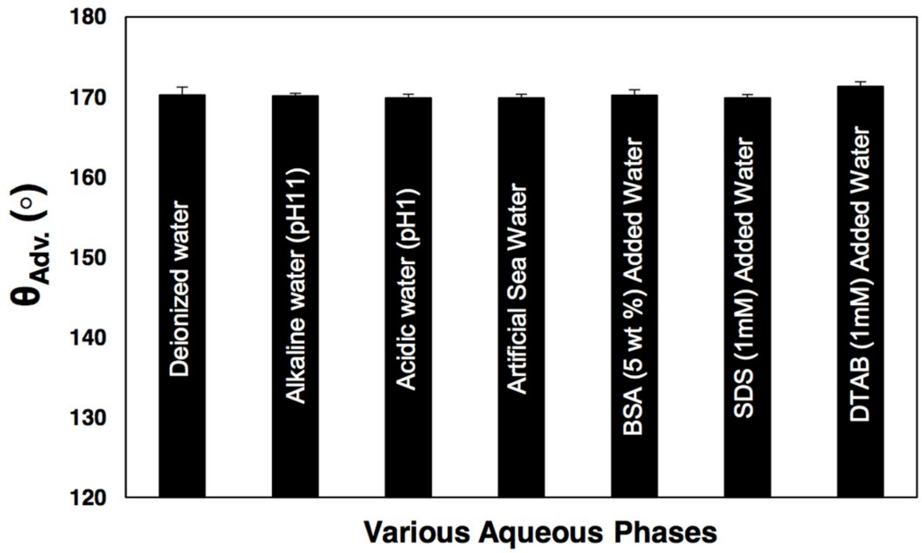

Fig. S11 The graph representing the advancing oil-contact angles under milli-Q water, alkaline-water (pH 11), acidic-water (pH 1), artificial sea-water, BSA-(5 wt.%) and surfactant- (SDS, DTAB ; conc. = 1mM each) contaminated water. The measurement was taken after 7days continuous exposure of the coating to the repulsive aqueous phase.

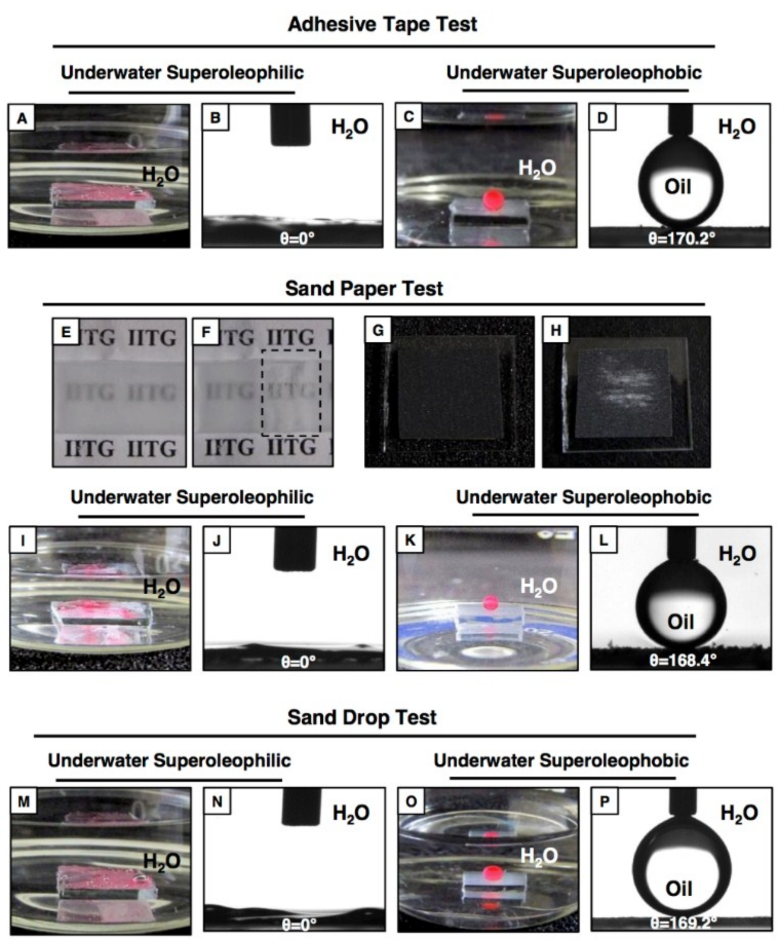

Fig. S12 A-D) Digital images (A, C) and contact angle images (B, D) are showing extremes of oil-wettability (superoleophilicity (A-B) and superoleophobicity (C-D)) under water after performing the adhesive tape test. E-F) Digital images are illustrating the physical change in the multilayer coated glass substrates in air before and after performing the sand paper abrasion test, the physically abraded area is marked with dotted box (F) and as a consequence of sand paper abrasion, the eroded powdery material are deposited/adhered on the sand paper (G-H). I-L) Digital images (I,K) and contact angle images (J,L) of beaded oil-droplet under water on Glu- (K-L) and

ODA- (I-J) treated multilayer of NC after the demonstration of sand paper abrasion test. M-P) Digital images (M,O) and contact angle images (N,P) showing the beading/wetting of oil-droplet on the Glu- (O-P) and the ODA- (M-N) treated multilayer of NC under water after performing the sand drop test.

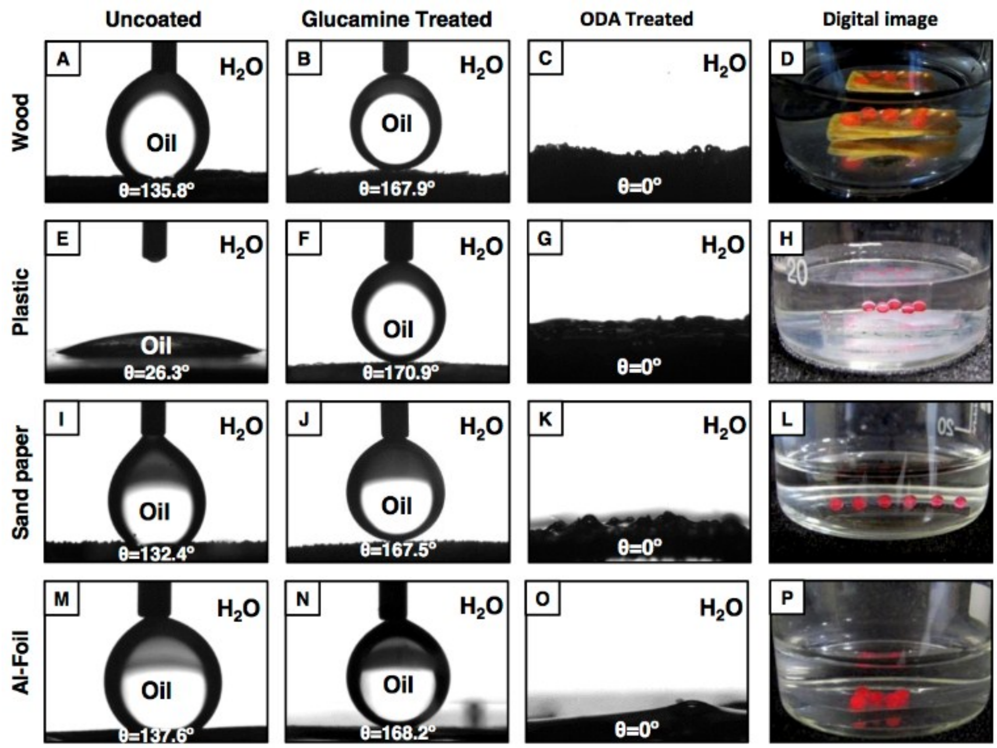

Fig. S13 A-P) Contact angle images (A-C, E-G, I-K, M-O) and digital images (D, H, L, P) illustrating the wetting of beaded oil-droplets on both the uncoated (A,E,I,M) and the multilayer coated (B,F,J,N: Glu-treated and C,G,K,O: ODA-treated) wood (B-D), plastic (F-H), sand paper (J-L) and aluminium foil (N-P) respectively.

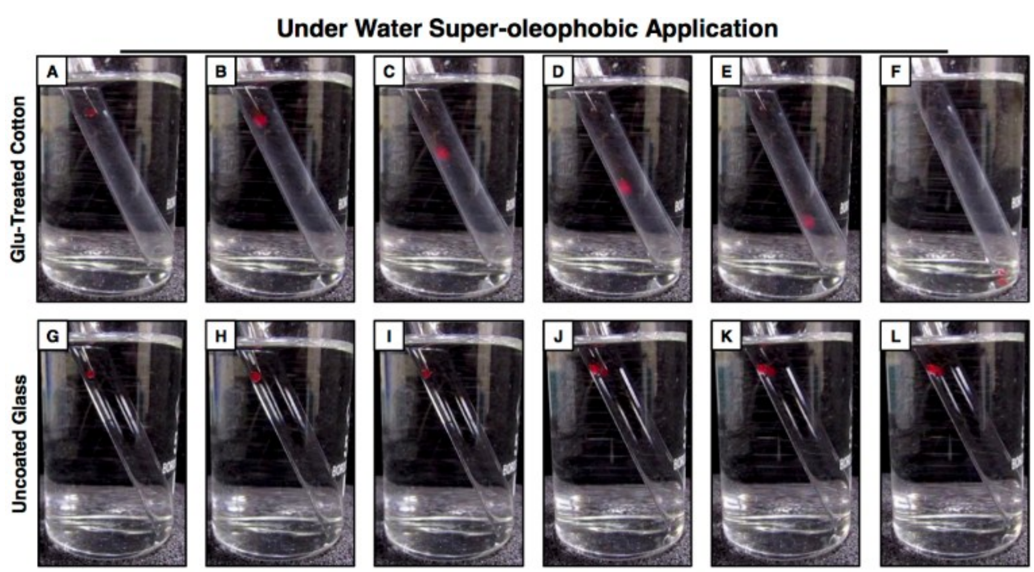

Fig. S14 A-F) Digital images of rolling oil-droplet (DCM; 8μl) through the tilted (~50°) glass tube under water, where the interior of the glass tube is decorated with under-water superoleophobic multilayer (glucamine-treated) coating, whereas (G-L) same oil-droplet pinned at the interior wall of the bare glass tube (at top) under water. No change is observed even after a day.

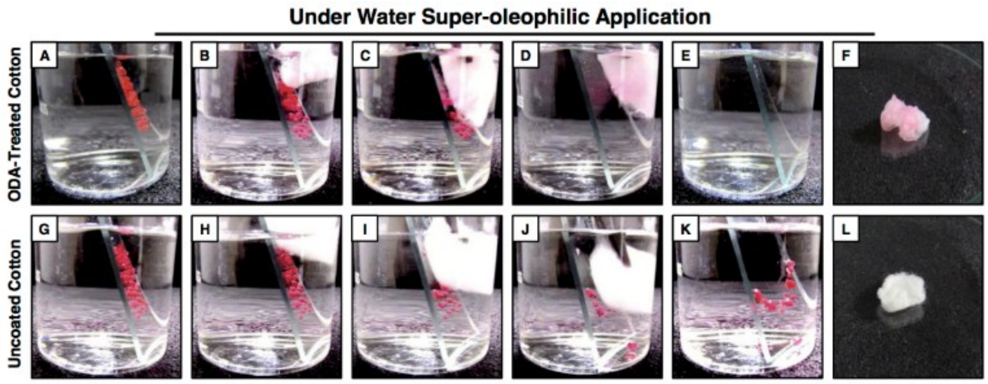

Fig. S15 A-F) Digital images showing instant collection of immobilized/adhered oil-droplets (DCM) from the bare glass surface under-water using multilayer coated (that post-modified with glucamine) superoleophilic-cotton, whereas, (G-K) uncoated and inherently under-water superoleophobic cotton is inappropriate to collect any trace of oil under water. F,L) Digital image of coated cotton (F) and uncoated cotton (L) after manual exposure to immobilized oil-droplets under water.